

System Identification
for the
Clipper Liberty C96 Wind Turbine

A THESIS
SUBMITTED TO THE FACULTY OF THE GRADUATE SCHOOL
OF THE UNIVERSITY OF MINNESOTA
BY

Daniel Showers

IN PARTIAL FULFILLMENT OF THE REQUIREMENTS
FOR THE DEGREE OF
MASTER OF SCIENCE

Peter J. Seiler, advisor

June 2014

© Daniel Showers 2014

Acknowledgments

I want to thank all those around me who supported me through the years. I would like to especially thank my wife, Lauren, my parents, my sister, and the Bruneau family for their support.

I also want to thank Pete Seiler for mentoring me through the process and for teaching me a lot along the way.

This material is based upon work supported by the National Science Foundation Graduate Research Fellowship under Grant No. 00039202. Any opinion, findings, and conclusions or recommendations expressed in this material are those of the authors and do not necessarily reflect the views of the National Science Foundation.

Abstract

System identification techniques are powerful tools that help improve modeling capabilities of real world dynamic systems. These techniques are well established and have been successfully used on countless systems in many areas. However, wind turbines provide a unique challenge for system identification because of the difficulty in measuring its primary input: wind. This thesis first motivates the problem by demonstrating the challenges with wind turbine system identification using both simulations and real data. It then suggests techniques toward successfully identifying a dynamic wind turbine model including the notion of an effective wind speed and how it might be measured. Various levels of simulation complexity are explored for insights into calculating an effective wind speed. In addition, measurements taken from the University of Minnesota's Clipper Liberty C96 research wind turbine are used for a preliminary investigation into the effective wind speed calculation and system identification of a real world wind turbine.

Contents

List of Figures	v
Chapter 1 Introduction	1
Chapter 2 Background	3
2.1 Wind Energy	3
2.2 The Wind Turbine	4
2.3 Wind Turbine Modeling	6
2.3.1 Simplified Turbine Model	6
2.3.2 High Fidelity Simulation Tools	7
2.4 Turbine Control	8
2.4.1 Region 2	9
2.4.2 Region 3	11
2.5 Power Coefficient Identification	12
Chapter 3 System Identification	15
3.1 Brief Description of CLMOESP Algorithm	15
3.2 Simplifications and Approach	17
3.3 Results	19

3.3.1	Uniform Inflow	19
3.3.2	Spatially Varying Inflow	20
Chapter 4	Effective Wind Speed	22
4.1	Approach	23
4.2	Results	24
Chapter 5	Conclusion	31
5.1	Future Work	32
	Bibliography	33
	Appendix A Appendices	36
A.1	Eolos Database Search Algorithm	36

List of Figures

2.1	Recent rapid growth of total installed wind power capacity [1]	3
2.2	Illustration of a typical wind turbine setup. From US Department of Energy	4
2.3	The Eolos Wind Research Station [2]	5
2.4	Free body diagram of wind turbine rotor.	6
2.5	Operating regions for Clipper Liberty C96.	9
2.6	C_p versus tip-speed ratio and pitch for Clipper Liberty C96. C_p values have been normalized to [-1 1] for proprietary reasons.	10
2.7	C_p versus tip-speed ratio at optimal blade pitch angle for Clipper Liberty C96. C_p values have been normalized for proprietary reasons.	11
2.8	Using data taken from Liberty C96 to solve Equation 2.5 for C_p . Data was taken for 35 minutes with mean wind speed of 8.42 m/s and 3% turbulence intensity. C_p values have been normalized.	13
2.9	Using simulated FAST data to solve Equation 2.5 for C_p . Data was simulated using the wind speed measured at the turbine from Figure 2.8 for the FAST wind speed input. C_p values have been normalized.	14
3.1	Block diagrams showing the difference in model to be identified.	18
3.2	Closed-loop system to be identified for Region 2 operation.	19
3.3	Uniform inflow wind speed results.	20

3.4	Spatially varying inflow wind speed results.	21
4.1	Closed-loop system to be identified for Region 2 operation using 2-D wind speed grid. n is the number of grid points ($ny \times nz$).	23
4.2	Identification and effective wind speed results using spatially uniform wind input to FAST.	25
4.3	Weights, ν_1 , across the rotor plane at low and high frequency for spatially uniform wind input to FAST.	25
4.4	Comparing FAST outputs when it is given hub height and full field wind speed inputs.	26
4.5	Effective wind speed results from spatially varying wind speed.	27
4.6	Weights, ν_1 , across the rotor plane at various frequencies for spatially varying wind input to FAST.	29

Nomenclature

Abbreviations and Acronyms

<i>CLMOESP</i>	Closed-Loop Multivariable Output Error State Space
<i>FAST</i>	Fatigue, Aerodynamics, Structures, and Turbulence
<i>TSR</i>	Tip Speed Ratio

List of Symbols

A	Rotor Swept Area, m^2
C_p	Power Coefficient, <i>unitless</i>
J	Rotor Inertia, $kg - m^2$
K	Generator Torque Controller Constant, $N - m/rpm^2$
P	Electrical Power Generated, <i>Watts</i>
P_{aero}	Power Available in the Wind, <i>Watts</i>
R	Rotor Radius, m
β	Blade Pitch Angle, <i>deg</i>
τ_{aero}	Aerodynamic Torque, $N - m$
τ_{gen}	Generator Torque, $N - m$
λ	Tip Speed Ratio, TSR, <i>unitless</i>
ω_r	Rotor Rotational Velocity, <i>rad/sec</i>
ρ	Air Density, kg/m^3

Chapter 1

Introduction

The development of renewable energy sources is important for our future because of the finite amount of fossil-based fuels and the environmental concerns associated with them. As a result, we have seen a large increase in the amount of installed capacity from renewable energy sources. One of the fastest growing renewable energy technologies is wind power. As more and more wind turbines are installed worldwide, understanding their dynamics and how to control the amount of power they can capture becomes essential for successful integration into the grid.

Current control strategies for wind turbines use simple techniques when taking the flexible dynamics of the turbine into consideration. They are designed using simple models and look-up tables that are only valid in steady state operation, and they are verified through high fidelity models such as the FAST (Fatigue, Aerodynamics, Structures, and Turbulence) wind turbine simulator maintained by the National Renewable Energy Laboratory (NREL). In order to design more advanced controllers to maximize energy and minimize structural loads, the dynamics of the wind turbine must be taken into consideration. Currently, FAST is used to create these dynamic models and to design advanced controllers for the simulation environment. However, there is a lack of verification methods for these high fidelity models, specifically in validating the flexible dynamics. There is a substantial difference between simulation and real world environments and, therefore, system identification is a useful approach to create dynamic models from real data.

Wind turbines present unique challenges to conventional system identification tech-

niques. The challenge with applying system identification techniques to wind turbines is the temporal and spatial unsteady nature of wind. These challenges have motivated my thesis which investigates the best way to measure wind speeds for wind turbine system identification.

In this thesis, I will present and motivate some of the challenges of verifying wind turbine models using both simulated and real data. I will then detail approaches taken to resolve these problems.

The following structure outlines the flow of the thesis. Chapter 2 provides an introduction to the wind turbine dynamic model and a background of current control strategies. In addition, Chapter 2 points out immediate challenges and shortcomings of using standard modeling techniques. Chapter 3 provides a brief theoretical background description of the subspace identification algorithm, closed-loop multi-variable output error state space (CLMOESP). In addition, it gives some results and insights gained from applying this method for various simulated levels of complexity. Chapter 4 introduces the notion of an effective wind speed and shows how the CLMOESP algorithm can be used to calculate it. Finally, Chapter 5 serves as a conclusion for the thesis and gives suggestions for future work.

Chapter 2

Background

Wind turbines are complex machines due to their large size and intricate interaction with their environment. The complicated nature of the turbine leads to complex, nonlinear dynamics. However, current wind turbine controller design depends upon a simplified model of the wind turbine, which is insufficient for advanced control design or system analysis.

2.1 Wind Energy

Wind energy is a young technology that has seen a rapid growth worldwide in the past 15 years as demonstrated in Figure 2.1.

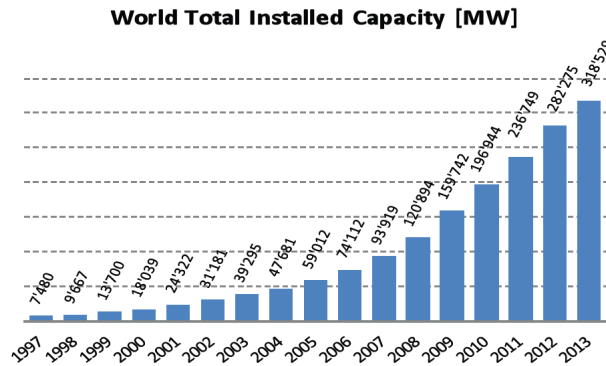


Figure 2.1: Recent rapid growth of total installed wind power capacity [1]

At the end of 2013, wind power was responsible for close to 4 percent of the total global

electricity generated, and 103 countries are now using wind power on a commercial basis. In some countries, wind power has reached over 20 percent of the electricity supply [1]. In the United States, wind accounts for about 32 percent of electricity from renewable sources [3].

Because wind power now holds a significant portion of generated electricity worldwide and is growing rapidly, it is important to increase the competitiveness of wind energy with other power sources by lowering the cost. This can be done by maximizing the power captured from a turbine and by lowering loads on turbines, extending their life. Smart design of control systems can achieve both of these objectives using advanced control design methods, which require detailed models. Data-driven modeling and verification can help provide such models.

2.2 The Wind Turbine

The most prevalent wind turbine design is a three bladed, horizontal axis wind turbine (HAWT). In this configuration, three evenly spaced blades rotate in a vertical plane. A yaw control system ensures that the plane of rotation is predominantly perpendicular to the incoming wind direction. HAWTs are the predominant configuration in the marketplace, and their use of active control makes them ideal for control research [4].

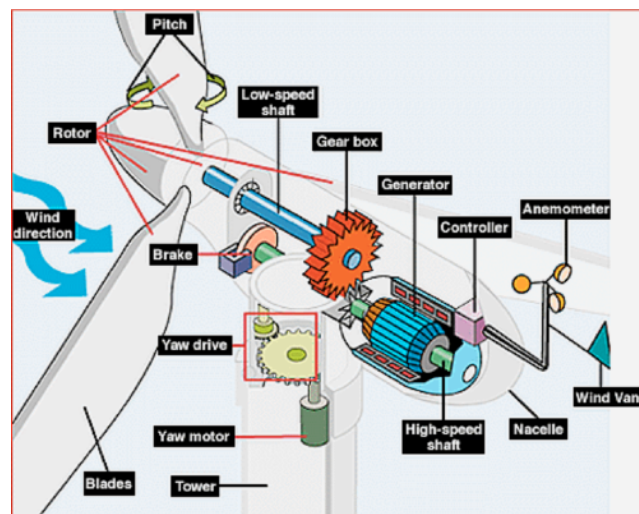


Figure 2.2: Illustration of a typical wind turbine setup. From US Department of Energy

Figure 2.2 shows, in more detail, the components of a typical HAWT. The incoming wind provides a lift force on the blades, which generates a torque and rotates the low-speed shaft. A gearbox increases the rotational rate of the low-speed side, making it suitable for electrical generation in the generator. The rotating shafts, gearbox, controller and generator are housed in the nacelle that sits atop the wind turbine tower. The nacelle also provides a mounting point for the rotor, which consists of the three blades and the hub that connects them. The blades are able to pitch along their main axis, controlling how much lift the blades are able to generate. The wind vane and anemometer provide wind speed and direction measurements to the controller [5].

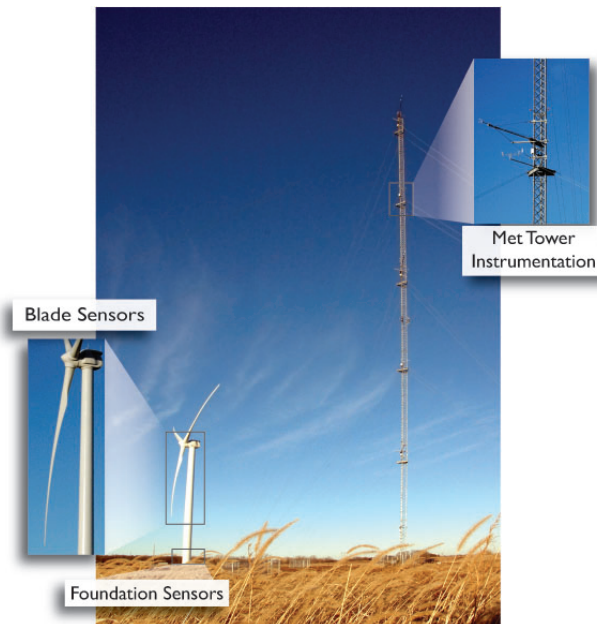


Figure 2.3: The Eolos Wind Research Station [2]

The University of Minnesota is a member of the Eolos wind energy research consortium, where industry and researchers can collaborate. One of the facilities that is a part of Eolos is the Wind Research Field Station in Rosemount, MN seen in Figure 2.3. The primary component of this research station is a Clipper Liberty C96 wind turbine. The C96 has a 96 meter rotor diameter and is rated to produce 2.5 MW of power. In addition to the sensors normally available on a wind turbine, this research station also has a meteorological tower, blade sensors, foundation sensors, and a portable LIDAR [2]. Measurements from these sensors are available to consortium members, providing a wealth of data to use for research purposes. Finally, all of the controller and high fidelity simulation files for the wind turbine are available for

research.

2.3 Wind Turbine Modeling

A wind turbine on its own is an unstable system. The wind develops a torque on the drive shaft and, if unchecked, will continually accelerate the drive shaft. There are various turbine designs that regulate the rotational speed using blade pitch and generator torque. Wind turbine blades can be designed as fixed or variable pitch and the rotor can also be designed to operate at either a fixed or variable speed. Most current machines that are rated for multi-MegaWatt power are variable-speed and variable-pitch because this provides the most degrees of freedom for a controller [4].

2.3.1 Simplified Turbine Model

The simplest way to model a turbine is as a stiff rotating dynamic system.

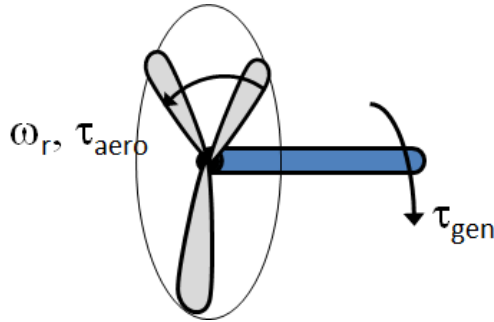


Figure 2.4: Free body diagram of wind turbine rotor.

A simple dynamic model can be developed using the free body diagram in Figure 2.4.

$$J\dot{\omega}_r = \tau_{aero} - \tau_{gen} \quad (2.1)$$

Equation 2.1 is simply a torque balance equation assuming a rigid rotor where J is the rotor inertia, τ_{aero} is the torque generated by the wind and τ_{gen} is the counteracting generator torque that produces power. The power available in the wind is given by

$$P_{wind} = \frac{1}{2}\rho Av^3 \quad (2.2)$$

where ρ is the air density, A is the rotor swept area, and v is the wind speed into the rotor plane. The aerodynamic power is given by

$$P = \tau_{aero}\omega_r \quad (2.3)$$

The relationship between the aerodynamic power and the power available in the wind is given by the non dimensional power coefficient, C_p , which varies depending on the rotor speed, wind speed and blade pitch angle.

$$C_p = \frac{P}{P_{wind}} \quad (2.4)$$

The power coefficient is a steady-state value describing how much of the power available in the wind the turbine is able to capture. The theoretical optimum value of the power coefficient is the Betz limit which is $\frac{16}{27}$ [5]. This limit is based upon a actuator disk, control volume analysis. Typical wind turbines achieve a maximum C_p value of 0.4 - 0.5 [5].

Using Equations 2.2, 2.3, and 2.4, 2.1 can be rewritten as

$$\dot{\omega}_r = \frac{1}{J} \left(\frac{1}{2} \rho A v^3 C_p \frac{1}{\omega_r} - \tau_{gen} \right) \quad (2.5)$$

Equation 2.5 is the simplified dynamic model of wind turbines used in control design.

2.3.2 High Fidelity Simulation Tools

While the simple model in Equation 2.5 is used for conventional turbine control design, high fidelity simulation tools are needed to verify these designs. Two of the more popular commercially available wind turbine simulation software packages are Bladed from DNV GL [6] and FAST (Fatigue, Aerodynamics, Structures, and Turbulence) from the National Renewable Energies Laboratory (NREL) [7].

FAST was used for all simulations in this thesis because it is freely available for download. The flexibility and capabilities of the FAST software are convenient for wind turbine controller design. It allows the user to activate up to 15 different blade and tower structural bending modes. It also allows the user to input a custom wind

profile that can be time and/or spatially varying. Alternatively, it can generate turbulent wind profiles based on user inputted turbulence statistics. Finally, FAST can generate linearized wind turbine models around a given wind speed.

While complex turbine models like FAST are great tools for wind turbine design and analysis, it is important to verify these models using real data. Differences between the simulation environment and the real operating conditions of the turbine or from turbine to turbine could include

- Differences in material properties
- Differences in manufacturing
- Differences between local soil or foundation characteristics
- Operational effects like icing of the blades or wear and tear on gears and actuators
- Modeling assumptions or simplifications

Using real data can help identify a more accurate model for each wind turbine in its operating environment. In particular, it is useful to verify the linearized models because they can be used for advanced control design.

2.4 Turbine Control

The simple, one state model shown in Equation 2.5 is the basis on which current control strategies are built. Wind turbine controllers are designed to maximize power while minimizing the loads on the structure. The two control degrees of freedom are the blade pitch angle, β , and the generator torque, τ_{gen} .

In typical controllers like the one on the Liberty C96, these two goals are accomplished by dividing the turbine operating modes into distinct regions based on wind speed [4].

Figure 2.5 shows the operating regions for the Clipper Liberty C96. Below the cut-in wind speed (3 m/s), the turbine is not generating any power because the power in the wind is low relative to system losses. This is referred to as Region 1. In Region 2, between the cut-in and rated wind speeds (3-11 m/s), the controller's goal is to

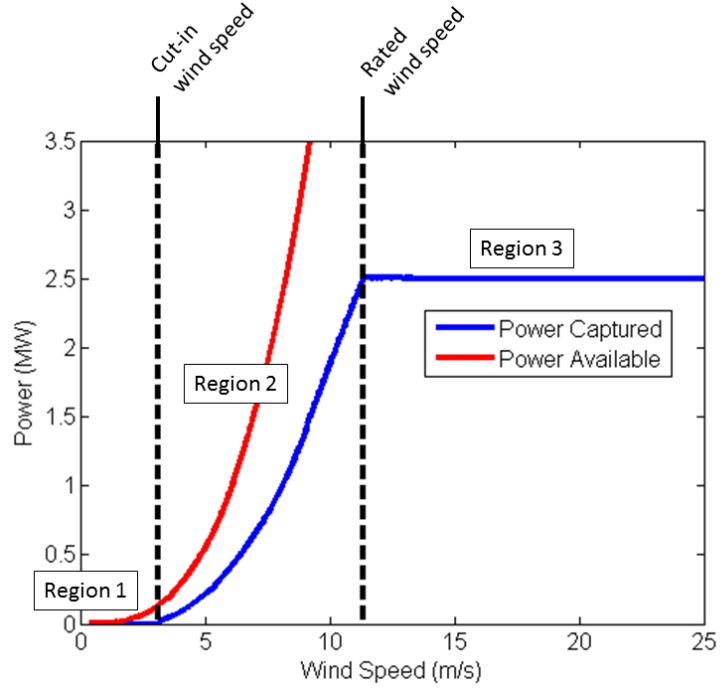


Figure 2.5: Operating regions for Clipper Liberty C96.

maximize the power captured. Above the rated wind speed, the controller maintains the rated power of the wind turbine. Finally, if the wind speed gets above 25 m/s, the turbine does not run to avoid the high loads associated with those extreme wind speeds. Certain proprietary techniques are used to blend these regions together so as to avoid constantly switching control strategies.

2.4.1 Region 2

In order to maximize the power captured, wind turbines need to extract as much power out of the wind as possible. From Equation 2.4, this is the same as operating at the highest C_p value possible. The power coefficient is a function of the blade pitch angle, β , and the tip-speed ratio, λ , which is a non dimensional value defined as the blade tip's speed divided by the wind speed:

$$\lambda = \frac{\omega_r R}{v} \quad (2.6)$$

where R is the rotor radius. As stated earlier, $C_p(\lambda, \beta)$ is a steady-state property of

the wind turbine. By obtaining C_p values at various tip-speed ratio and blade pitch angle combinations, a two-dimensional look-up table (3-D surface) is created. The C_p values for the power curve can be computed by providing a steady wind input to the FAST model, letting the simulation run to steady-state, and computing C_p from Equation 2.4. An example of the three-dimensional power curve for the Clipper Liberty C96 is shown in Figure 2.6.

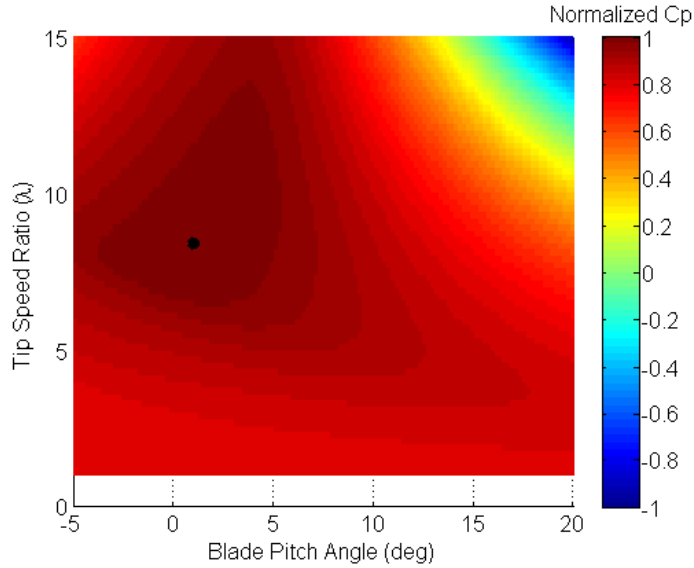


Figure 2.6: C_p versus tip-speed ratio and pitch for Clipper Liberty C96. C_p values have been normalized to $[-1 \ 1]$ for proprietary reasons.

As seen in Figure 2.6, the power coefficient does have a maximum value. In order to maximize power captured, the controller will attempt to stay at this maximum C_p value by maintaining the optimal tip-speed ratio and blade pitch angle. Typically, this is accomplished by keeping the blade pitch constant at its optimal value and adjusting the generator torque to track the optimal tip-speed ratio.

In order to stay near the peak power coefficient, turbines employ a nonlinear torque control law

$$\tau_{gen} = K\omega_r^2 \tag{2.7}$$

where K is a constant given by

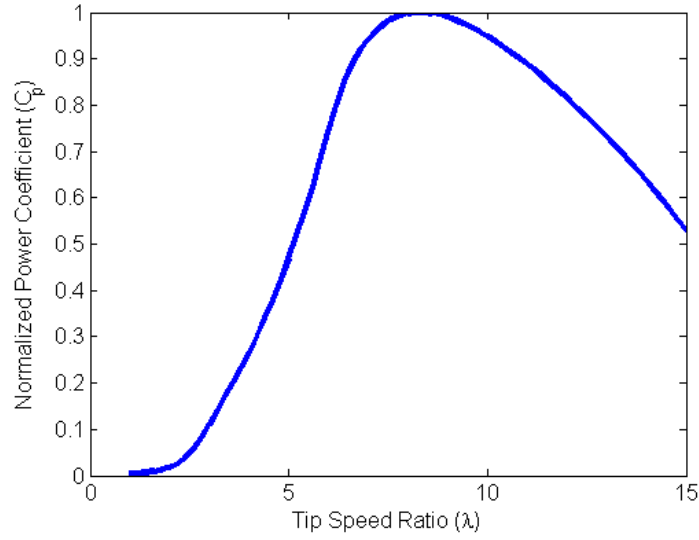


Figure 2.7: C_p versus tip-speed ratio at optimal blade pitch angle for Clipper Liberty C96. C_p values have been normalized for proprietary reasons.

$$K = \frac{1}{2}\rho AR^3 \frac{C_{p,max}}{\lambda_{opt}^3} \quad (2.8)$$

Therefore, in Region 2, Equation 2.5 becomes

$$\dot{\omega}_r = \frac{1}{2J}\rho AR^3 \omega_r \left(\frac{C_p(\lambda, \beta)}{\lambda^3} - \frac{C_{p,max}}{\lambda_{opt}^3} \right) \quad (2.9)$$

It can be seen from Equation 2.9 that in steady-state the turbine will converge to the optimal power capture (λ converges to λ_{opt}) [4].

This control law is simple and easily implemented, only needing a rotor speed sensor, which is why it is popular in industrial turbines. However, it requires accurate knowledge of the turbine's optimal operating point ($C_{p,max}$ and λ_{opt}), which is difficult to verify in practice.

2.4.2 Region 3

In Region 3, the wind speed is high enough that the turbine can produce its rated power. In this wind regime, the controller's goal is to provide a constant, rated power

to the grid. To do this, the generator torque is held constant at its rated value and the blades are pitched (decreasing C_p) to maintain the rated rotor speed. From Equation 2.3, by maintaining constant torque and rotor speed at their rated values, the turbine will produce its rated power.

The blade pitch controller typically uses PID or PI techniques to track the rated rotor speed using the rotor speed sensor for feedback [4]. Some commercial wind turbines allow each of the three blades to pitch independently for more control authority which helps to take rotational dependencies into account, called individual pitch control (IPC).

2.5 Power Coefficient Identification

Calculating K in Equation 2.8 requires accurate knowledge of the C_p versus λ curve from Figure 2.7. As a first approach, solving Equation 2.5 for C_p as 2.10 seems like it may give insight into the true nature of the C_p curve under relatively steady wind conditions because all values are known or directly measured from the wind turbine except for C_p .

$$C_p = (J\dot{\omega}_r + \tau_{gen}) \frac{2\omega_r}{\rho v^3 A} \quad (2.10)$$

Given that the rotor radius is 48 m, the rotor area is about 7240 m². The air density is measured on the turbine and was 1.257 $\frac{kg}{m^3}$. Data such as rotor speed, generator torque and wind speed are collected at 20 Hz. For calculating C_p , the 20 Hz measured data is averaged to 1 Hz data for rotor speed and generator torque. For wind speed, the 20 Hz data is outputted as a 60 second averaged time series. Finally, $\dot{\omega}_r$ is calculated simply using a difference method $\frac{\Delta\omega_r}{\Delta t}$. The theoretical C_p curve from Figure 2.7 can be used as a comparison. This theoretical table look-up is created using an NREL software called WT_PERF that is a companion software package to FAST. WT_PERF creates the theoretical look-up table of C_p values by running the turbine to steady state at different tip-speed ratios and blade pitch angles and calculating C_p using 2.4.

As seen in Figure 2.8, this approach for calculating the C_p values using real data does not produce meaningful results. Although the tip-speed ratio remains relatively constant as it should in Region 2, the C_p values do not match well with the theoretical power coefficients.

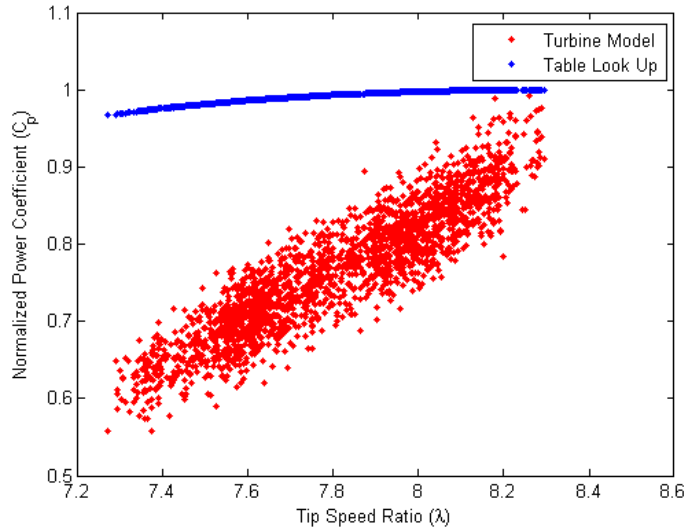


Figure 2.8: Using data taken from Liberty C96 to solve Equation 2.5 for C_p . Data was taken for 35 minutes with mean wind speed of 8.42 m/s and 3% turbulence intensity. C_p values have been normalized.

Equation 2.5 is highly dependent upon the wind speed. On the Clipper Liberty C96, as on most commercial wind turbines, the anemometer is measuring the wind speed behind the rotor plane (Figure 2.2) where the flow has been disturbed by the blades resulting in an inaccurate measurement. In addition, the anemometer is measuring the wind speed at one location, but the wind turbine is driven by wind speeds across a large rotor diameter. Therefore, using a point measurement may not be the best way to calculate a C_p curve. Finally, Equation 2.5 does not take any bending modes into account, which could be another source of inaccuracies.

In order to narrow down the source of error, FAST was used to simulate the turbine with no bending modes activated and a spatially uniform wind profile.

Figure 2.9 is much improved over the results from Figure 2.8. This shows the importance of knowing the true wind speed and having a stiff turbine. Although these simulation results are improved, there are still sources of error even in an ideal simulation environment. Therefore, it seems that using a steady state C_p value does not accurately capture the wind turbine dynamics. For model verification, it may be better to perform more of a black box system identification approach rather than fitting parameters to a given model.

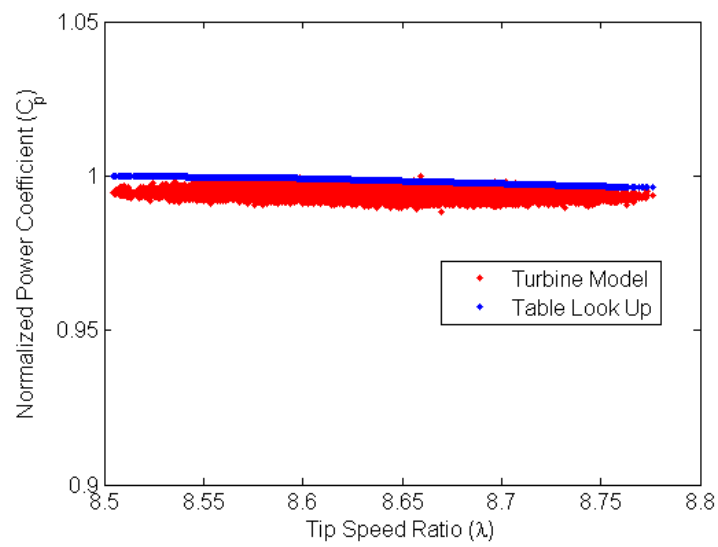


Figure 2.9: Using simulated FAST data to solve Equation 2.5 for C_p . Data was simulated using the wind speed measured at the turbine from Figure 2.8 for the FAST wind speed input. C_p values have been normalized.

Chapter 3

System Identification

Wind turbines present several unique challenges to conventional system identification techniques such as those described in [8]. First, wind turbines cannot be operated in open-loop due to the risk of instability and excessive loads. Second, there is no control over the primary system input, wind. This makes it impossible to set up a proper open-loop test. There have been many approaches to performing system identification on wind turbines including [9], [10], [11], [12], [13]. In order to address the previously stated issues, this thesis will focus on the closed-loop multi-variable output error state space (CLMOESP) system identification algorithm. This algorithm was chosen because it takes the closed-loop operation of the turbine into account. Next, it is a subspace identification technique meaning it takes time series data as inputs, which is the form of the data available from Eolos. It also has the advantage of identifying multi-input multi-output (MIMO) systems, which is what the wind turbine is. Finally, this algorithm is available for MATLAB from [14] and gave better results compared to other closed-loop subspace identification methods.

3.1 Brief Description of CLMOESP Algorithm

The following discrete-time, state-space system is considered:

$$\begin{aligned}x_{k+1} &= Ax_k + Bu_k + w_k \\ y_k &= Cx_k + Du_k + v_k\end{aligned}\tag{3.1}$$

with $A \in \mathbb{R}^{n \times n}$, $B \in \mathbb{R}^{n \times n_u}$, $C \in \mathbb{R}^{n_y \times n}$, and $D \in \mathbb{R}^{n_y \times n_u}$. The vectors $x_k \in \mathbb{R}^n$, $u_k \in \mathbb{R}^{n_u}$, and $y_k \in \mathbb{R}^{n_y}$ form the state, input, and output vectors respectively. The signals $w_k \in \mathbb{R}^n$ and $v_k \in \mathbb{R}^{n_y}$ are the process and measurement noise respectively and are uncorrelated, zero-mean, and white Gaussian. Equation 3.1 can be rewritten in the one-step-ahead predictor form

$$\begin{aligned} x_{k+1} &= \tilde{A}x_k + \tilde{B}u_k + Ky_k \\ y_k &= Cx_k + Du_k + e_k \end{aligned} \quad (3.2)$$

where $K \in \mathbb{R}^{n \times n_y}$ is a Kalman gain, $e_k \in \mathbb{R}^{n_y}$ is the innovation sequence, $\tilde{A} = A - KC$ and $\tilde{B} = B - KD$.

A data sequence, y_k , can be written in block Hankel form:

$$Y_{i,s,N} = \begin{bmatrix} y_i & y_{i+1} & \cdots & y_{i+N-1} \\ y_{i+1} & y_{i+2} & \cdots & y_{i+N} \\ \vdots & \vdots & \ddots & \vdots \\ y_{i+s-1} & y_{i+s} & \cdots & y_{i+N+s-2} \end{bmatrix} \quad (3.3)$$

When $s = 1$, it shall be denoted as $Y_{i,N}$.

The goal of the CLMOESP algorithm is to identify the A , B , C , D , and K matrices given input/output data sequences u_k and y_k . The first step in the CLMOESP algorithm is solving for the innovation sequence, e_k . Using the block Hankel notation for p past data points, the output equation from 3.2 can be written as

$$Y_{p,N-p} = C\mathcal{K}^{(p)}Z_{0,p,N-p} + DU_{p,N-p} + E_{p,N-p} \quad (3.4)$$

assuming p is chosen large enough that $\tilde{A}^p \approx 0$. In 3.4, $\mathcal{K}^{(p)}$ is an extended controllability matrix and is defined as

$$\mathcal{K}^{(p)} = \left[\tilde{A}^{p-1}\tilde{B}, \tilde{A}^{p-2}\tilde{B}, \dots, \tilde{B} \right] \quad (3.5)$$

where $\bar{B} = \begin{bmatrix} \tilde{B} & \mathcal{K} \end{bmatrix}$ and the block Hankel matrix Z_{0,p,N_p} formed from the data sequence

$$z_k = \begin{bmatrix} u_k^\top & y_k^\top \end{bmatrix}^\top \quad (3.6)$$

The innovation sequence is then solved for from the minimization problem

$$\min_{C\mathcal{K}^{(p)}, D} \left\| Y_{p,N_p} - \begin{bmatrix} C\mathcal{K}^{(p)} & D \end{bmatrix} \begin{bmatrix} Z_{0,p,N_p} \\ U_{p,N_p} \end{bmatrix} \right\|_F^2 \quad (3.7)$$

Once the innovation sequence has been determined, the algorithm follows the ordinary MOESP identification scheme [15]. First, an extended observability matrix is estimated using an orthogonal projection matrix on a block Hankel version of the innovation representation of the data equation. From this extended observability matrix, the state matrices A and C can be obtained. Finally, the state matrices B, D, and K can be calculated by solving a least squares problem. For more details on the CLMOESP and MOESP algorithms see [15], [16], [17], [18].

3.2 Simplifications and Approach

The CLMOESP algorithm was used in [11] for identification of wind turbine models using the aerodynamic torque and force as inputs calculated from Equation 2.5. This assumes that the C_p curve is known. The reason it was done that way was to avoid the nonlinearities of the wind turbine model and perform the identification algorithm on an arbitrary data sequence. Otherwise, it would be necessary to perform the algorithm on a data set that remains close to a given operating point for the system to maintain approximately linear behavior. Because the Eolos wind station is continuously collecting data, it is not hard to find adequately long sets of data that exhibits relatively consistent behavior. The algorithm used to find these appropriate data sequences within the Eolos database can be found in Appendix A.1. Additionally, the purpose of identifying dynamic models is to design advanced controllers, which require linear models, so the model will have to be linearized anyway. For these reasons, the CLMOESP algorithm was used as more of a black box technique with wind speed, blade pitch angle, and generator torque as inputs and rotor speed and tower

acceleration as outputs. In this way, the CLMOESP algorithm will be performed at each wind speed to obtain a series of linear models valid across a range of wind speeds.

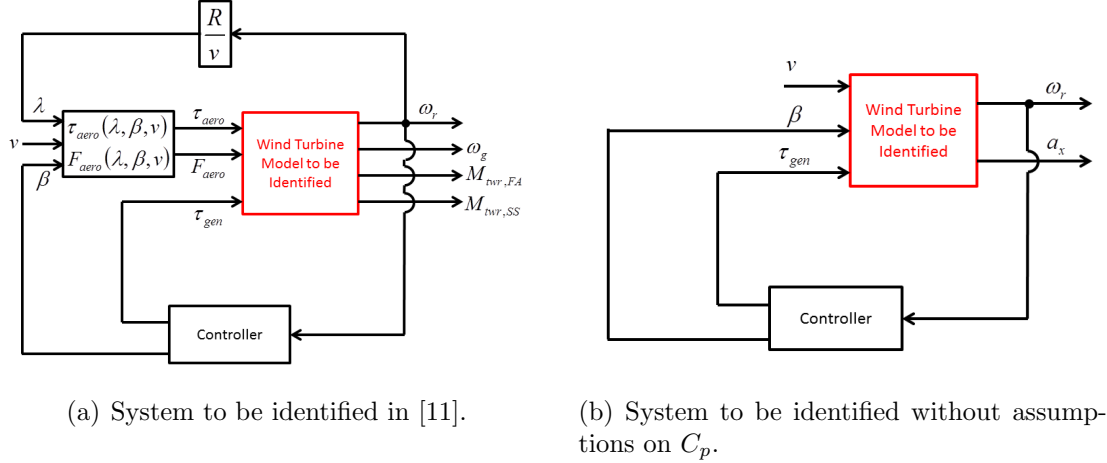


Figure 3.1: Block diagrams showing the difference in model to be identified.

The difference between the approaches can be better visualized in 3.1. The algorithm from [11] has the advantage that it can be used on an arbitrary data series and then linear models can be obtained by linearizing the nonlinear aerodynamic force and torque equations about the operating point. However, it assumes knowledge of the C_p curve. The approach presented in this thesis has the disadvantage that an appropriate data series where the wind turbine is operating close to some operating point must be found. Although not always possible, it is not hard to find such data series with the Eolos database, and the advantage is that no assumptions about the turbine dynamics must be made.

Another advantage of identifying the whole nonlinear system about an operating point is that it can be further simplified by restricting the operating point of the turbine to either Region 2 or Region 3 operation. This is advantageous because, for example, in Region 2, blade pitch is not used and the control law for generator torque, Equation 2.8, is easily linearizable as $\delta\tau_{aero} = 2K\delta\omega_r$ so that the open-loop system can be determined from identifying the closed-loop system. This further simplification of Region 2 operation finally brought the identified system to that seen in Figure 3.2.

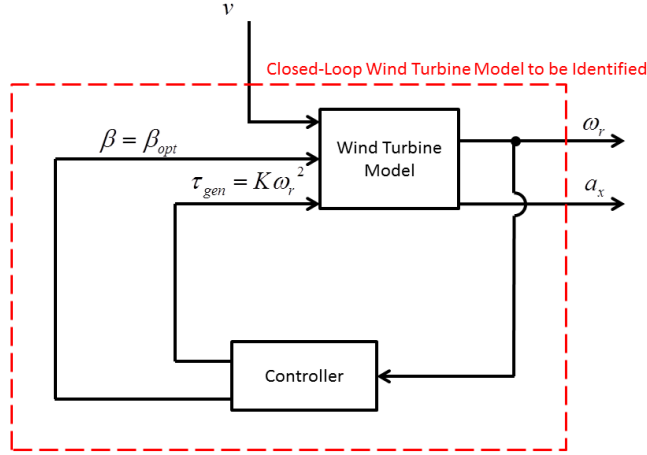


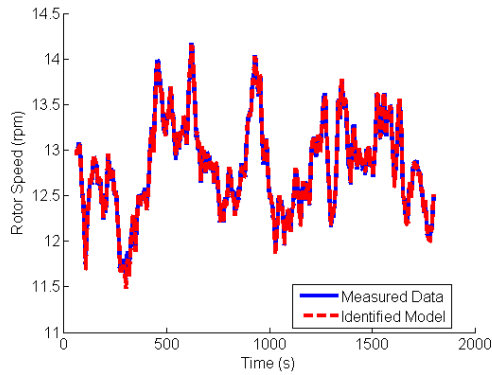
Figure 3.2: Closed-loop system to be identified for Region 2 operation.

3.3 Results

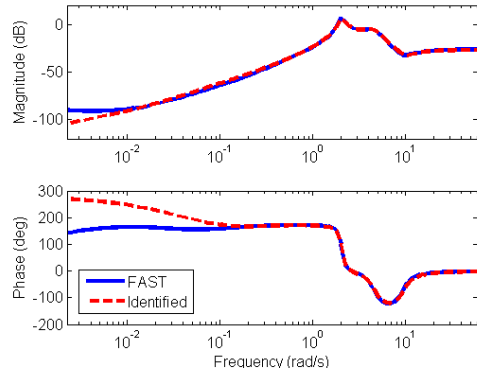
3.3.1 Uniform Inflow

To prove the viability of this approach, FAST was used to generate simulated data with the first fore-aft tower bending degree of freedom and the first flapwise blade degree of freedom activated resulting in a 10 state linearized model. In this way, the identified linear model could be compared to the FAST linearized model. The wind speed input to FAST was uniform across the rotor plane with a turbulence intensity of 5% and a mean wind speed of 7.75 m/s. This ensured that the turbine would operate in Region 2 for the duration of the simulation and provided enough excitement to identify the structural modes of the turbine.

For this simple simulated example, a 10 state system was identified because that is the number of states in the FAST linearized model allowing for easy comparison between the two. The algorithm was able to replicate the time series data with a 95.4% fit of the rotor speed data shown in Figure 3.3 (a) and a 80.4% fit of the acceleration data. The identified system also matched well in the frequency domain for both the rotor speed and acceleration seen in Figure 3.3 (b). The algorithm was able to accurately identify the modes but does not match well at low frequencies because the FAST linearized model is not accurate at low frequencies. Because FAST creates



(a) Rotor speed verification.



(b) Bode plot of wind speed, v (m/s), to nacelle fore-aft acceleration, a_x (m/s^2).

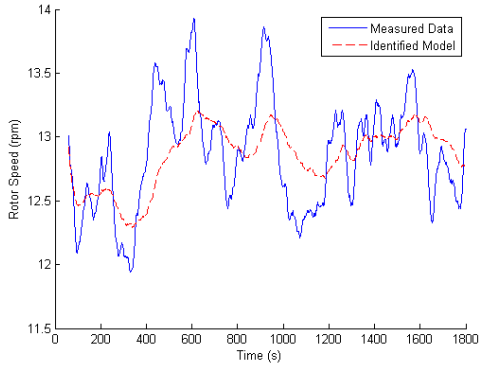
Figure 3.3: Uniform inflow wind speed results.

the linear model by numerically linearizing the FAST model about a steady state operating point, its linearized model has a pole very close to zero when it should be exactly zero [19]. This slight numerical issue causes the FAST linearized model to be inaccurate at low frequencies. Therefore, the algorithm is able to identify the linear turbine model accurately in the time and frequency domains for a spatially uniform wind speed input.

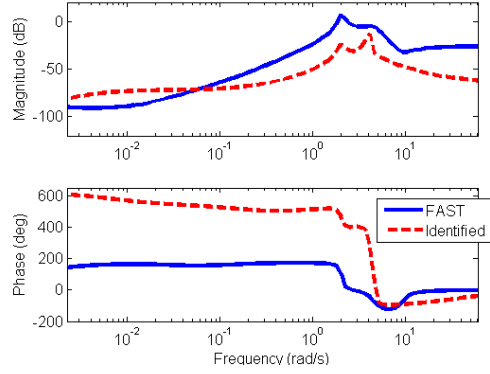
3.3.2 Spatially Varying Inflow

In order to make the simulation more realistic, the next step was to make the wind input vary across the rotor plane to mimic real operating conditions. The mean hub height wind speed was kept at 7.75 m/s, but the wind speed varied stochastically horizontally across the rotor plane and followed the wind shear log law vertically across the rotor plane. Using these specifications, the wind speed was defined on an evenly spaced 11×11 grid. For the identification algorithm, the hub height wind speed was used as the input because this is where the anemometer on the real wind turbine would measure the wind speed.

With the addition of the spatially varying wind input, the algorithm is no longer able to accurately identify the wind turbine model with only a 19.1% match of the rotor speed time series data seen in Figure 3.4 (a) and a 0.7% match of the tower acceleration time series data. Likewise, the frequency domain data did not match as seen in Figure 3.4 (b). This result indicates that an appropriate wind speed



(a) Rotor speed verification.



(b) Bode plot of wind speed, v (m/s), to nacelle fore-aft acceleration, a_x (m/s^2).

Figure 3.4: Spatially varying inflow wind speed results.

measurement is the key to successful identification of the wind turbine model. When the wind speed at all points is known as in Figure 3.3, the algorithm accurately identifies the model. However, when the wind speed varies at all points in the rotor plane but only one wind speed is used as an input as in Figure 3.4 and in the real system, the algorithm is no longer able to identify an accurate model. This begs the question of what the appropriate wind speed measurement should be for successful system identification when the wind speed varies at every point across the rotor plane.

Chapter 4

Effective Wind Speed

In [20], the term "effective wind speed" is coined to describe the ideal wind speed to measure defined in [5] as "the spatial average of the wind field over the rotor plane with the wind stream being unaffected by the wind turbine, i.e. as if the wind turbine was not there". While impossible to measure in practice, there have been many attempts to estimate the effective wind speed. For example, [20] uses a two step process to estimate the angular velocity and aerodynamic torque and, from the aerodynamic torque estimate, calculate an effective wind speed by inverting the aerodynamic model, Equation 2.3. Another approach presented in [21] is based on a continuous-discrete extended Kalman filter where the wind speed is a state modeled by turbulent and mean components. Yet another approach seen in [22] uses unknown input observer techniques to simultaneously estimate the effective wind speed and the power coefficient. There have been many other similar approaches to those presented here including [23], [24], [25], and [26]. However, what all of these approaches have in common is that they assume knowledge of the turbine dynamics. In order to construct the Kalman filters and unknown input observers, there must be a dynamic model of the wind turbine. Therefore, these approaches to calculating the effective wind speed are not of interest when trying to perform system identification. This section will explore measurement techniques that could be used to get the effective wind speed. In other words, if the wind speed could be measured at any point(s), where should it be measured and how could these point measurements be combined to get an effective wind speed that results in successful system identification.

4.1 Approach

By viewing effective wind speed as the wind speed that allows for the best model identification results, it makes sense to use the CLMOESP algorithm in calculating the effective wind speed. Therefore, the same CLMOESP algorithm used in 3 is used in estimating an effective wind speed. The difference is that, instead of using the hub height wind speed as the input, the full grid of wind speeds across the rotor plane are used as inputs. Therefore, there will be $n_y \times n_z$ inputs where n_y is the number of grid points in the y (horizontal) direction and n_z is the number of grid points in the z (vertical) direction. The slight difference in how the CLMOESP algorithm is used is visualized in 4.1.

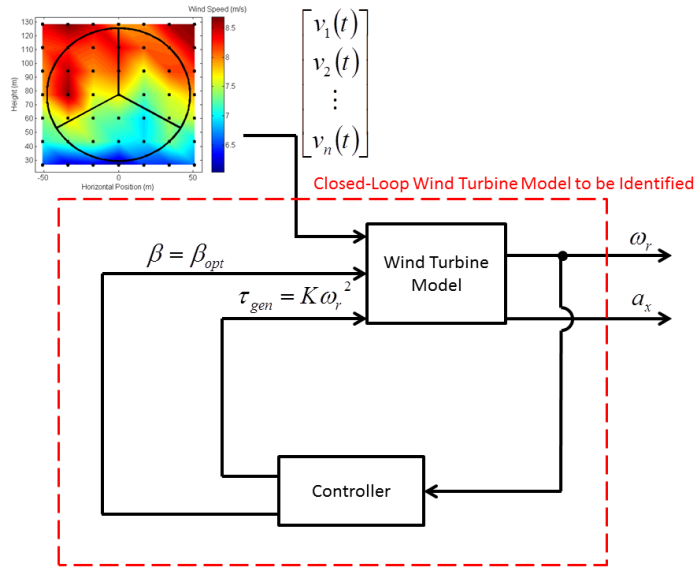


Figure 4.1: Closed-loop system to be identified for Region 2 operation using 2-D wind speed grid. n is the number of grid points ($n_y \times n_z$)

Because the Hankel matrices given in 3.3 grow quickly with the number of inputs and outputs, the biggest grid that the CLMOESP algorithm could handle was 11×11 , so that was the grid size used for testing the algorithm to get the finest grid and most detailed information. Using a 11×11 wind speed grid made the input, u , to the identified system a 121×1 vector at each time step. Therefore, the transfer function matrix, $G(s)$, that is identified from the input/output data will contain information about how much each wind speed location is weighted for the system dynamics. This transfer function matrix is 1×121 and can be evaluated at various frequencies. In

order to quantify this weight, a singular value decomposition can be performed at each frequency on the identified transfer function matrix, $G(j\omega)$.

$$G(j\omega) = U(j\omega)\Sigma(j\omega)V(j\omega)^* \quad (4.1)$$

The matrix of singular values, Σ , is a 1×121 vector and the $(1, 1)$ entry is nonzero while the remaining entries are zero. By decomposing the $G(s)$ matrix in this way, the weights at each grid point can be evaluated by looking at the first column of the $V(j\omega)$ matrix at various frequencies. An effective wind speed can be calculated as

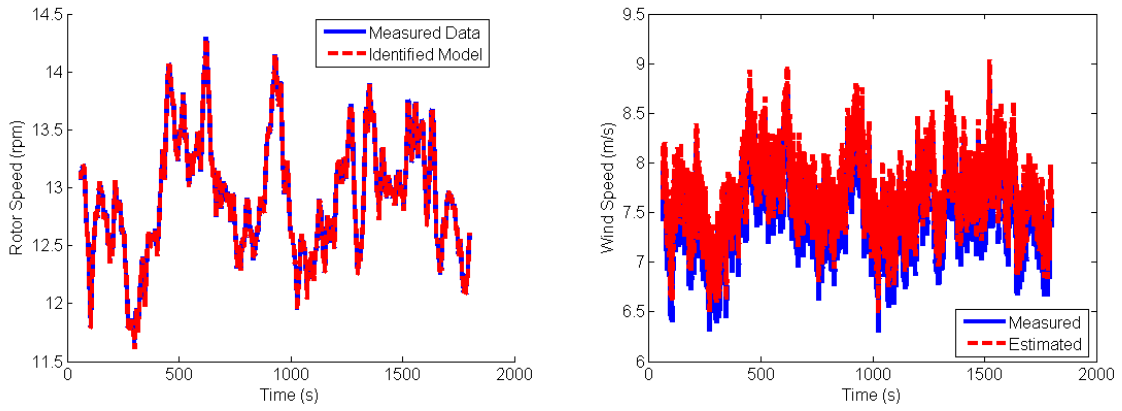
$$v_{eff}(j\omega) = \nu_1(j\omega)^T \begin{bmatrix} v_1(j\omega) \\ v_2(j\omega) \\ \vdots \\ v_n(j\omega) \end{bmatrix} \quad (4.2)$$

where ν_1 is the first column of the V matrix in Equation 4.1 corresponding to the only real singular value of $G(s)$. The values of ν_1 show how the wind speeds at different grid points are weighted to combine to form an effective wind speed. These weights indicate where it is most important to measure the wind speed if you could measure it anywhere across the rotor plane. Because $G(s)$ is decomposed at various frequencies, ν_1 is different at every frequency. Studying these weights across frequencies can give better insight into how the effective wind speed depends on frequency.

4.2 Results

In order to test this approach on a simple example, a full 11×11 wind field was created and given to the CLMOESP algorithm as the inputs. However, only the hub height grid point was given as an input to the FAST simulation so that FAST used the hub height wind speed as a uniform wind speed across the rotor plane. For this simple example, the algorithm should not only be able to identify a system that matches the input/output data but also identify that the hub height wind speed is the effective wind speed.

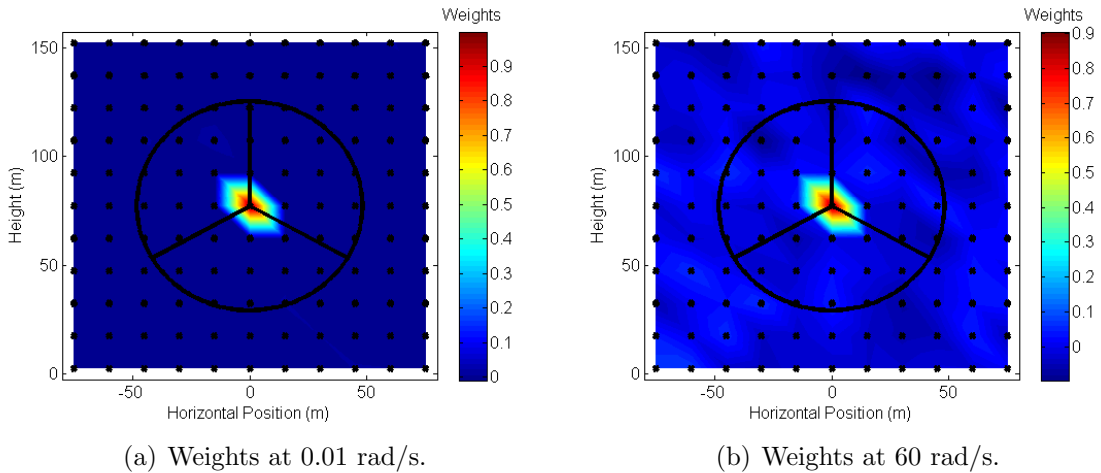
Figure 4.2 shows that this approach of using the full wind speed grid as inputs and using a singular value decomposition on the identified $G(s)$ matrix to determine the



(a) Rotor speed from identified model matches (b) Effective wind speed from 4.2 matches with well with measured rotor speed. wind speed input.

Figure 4.2: Identification and effective wind speed results using spatially uniform wind input to FAST.

effective wind speed works for the simple example. The algorithm is able to correctly match the rotor speed output in the time domain with a 98.59% fit (Figure 4.2 (a)) and the effective wind speed is the hub height wind speed as it should be (Figure 4.2 (b)).



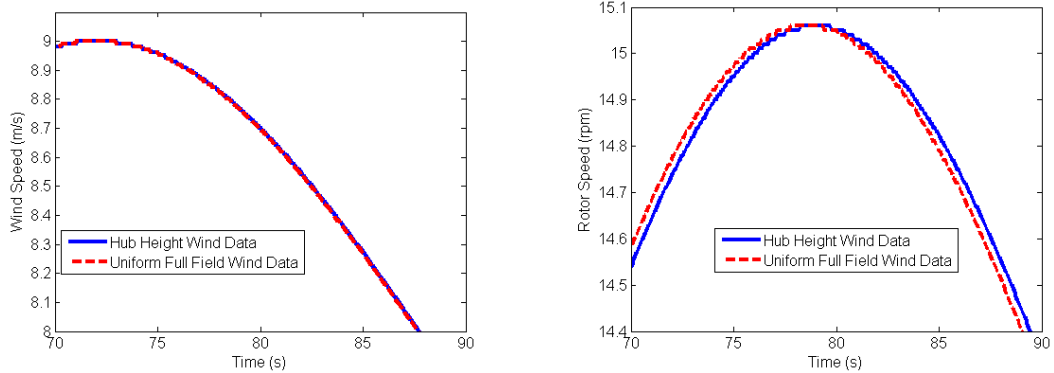
(a) Weights at 0.01 rad/s.

(b) Weights at 60 rad/s.

Figure 4.3: Weights, ν_1 , across the rotor plane at low and high frequency for spatially uniform wind input to FAST.

Finally, the weights from ν_1 show that the hub height wind speed is weighted by far the most as expected (Figure 4.3) and that the weighting does not vary with frequency.

The next step was to perform the same identification algorithm, but with the full 11×11 wind field used as the input for the FAST simulation. An additional step had to be taken in order to analyze the data from the full wind field simulation. For processing full field wind inputs, FAST uses software called TurbSim to simulate the flow field around the turbine. TurbSim initializes at a delayed time so that the wind is fully defined around the turbine before starting the simulation. This time delay is equal to the grid width divided by the mean wind speed [27]. Because of this, all of the FAST outputs are delayed by a time constant compared to the uniform hub height wind speed simulation. However, the time constants for the wind speed, rotor speed and nacelle acceleration are different. These different time delays had to be accounted for when running the algorithm so that the data aligned and the model could be identified.



(a) Wind speed offset between hub height wind speed and full field wind speed FAST inputs.

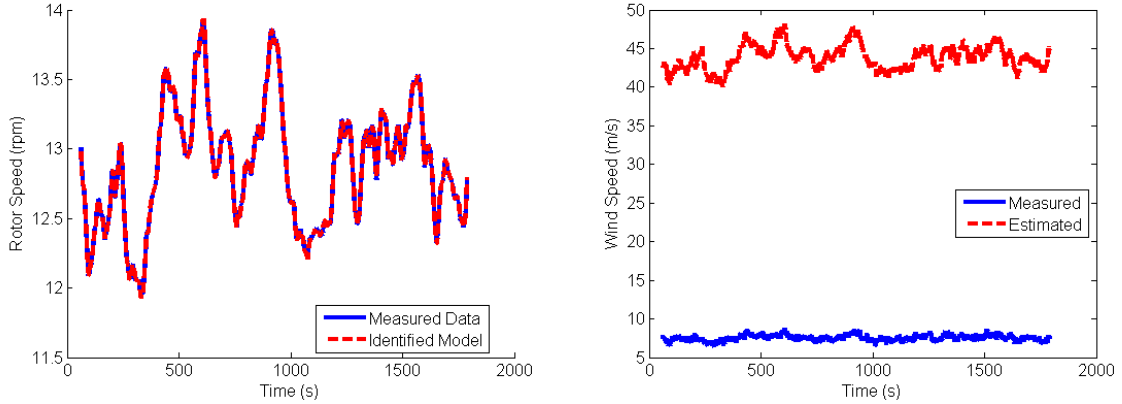
(b) Rotor speed offset between hub height wind speed and full field wind speed FAST inputs.

Figure 4.4: Comparing FAST outputs when it is given hub height and full field wind speed inputs.

The different delays seen in the wind speed and rotor speed are illustrated in Figure 4.4. The plots seen in Figure 4.4 compare the FAST outputs for when a uniform, hub height wind file is input to FAST and when a spatially uniform, gridded wind file is input to FAST. Both data sequences have had the same time delay taken out $\frac{GridWidth}{AvgWindSpeed}$, which is about 6.5 seconds. Removing this delay aligns the wind speed data series, but not the rotor speed series. The delays are different by about 0.4 seconds, and this had to be removed before performing system identification using the full gridded wind field as inputs. The nacelle acceleration and rotor speed were both delayed by the same amount. Determining the physical reason for this delay is

an area of future work.

After removing this time delay, the CLMOESP algorithm was run using an 11×11 wind field as input and the FAST outputs from using that wind field as the input to the simulation.

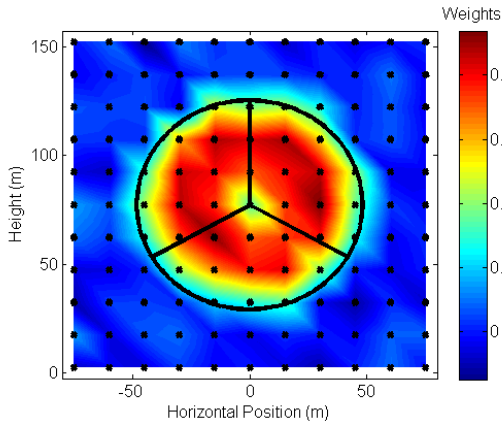


(a) Rotor speed from identified model matches well with measured rotor speed. (b) Effective wind speed from 4.2 at 0.01 rad/s compared with hub height wind speed measurement.

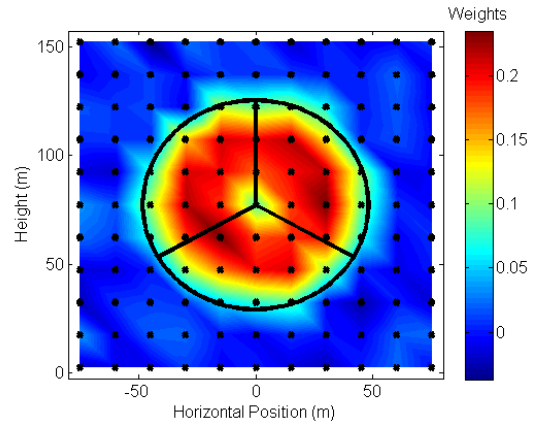
Figure 4.5: Effective wind speed results from spatially varying wind speed.

Figure 4.5 (a) shows that this approach was successful at matching the rotor speed measured in FAST with a 98.55% fit. Figure 4.5 (b) shows that the calculation of effective wind speed from 4.2 using the singular value decomposition at 0.01 rad/s gives nonsensical results. The effective wind speed calculation produced similar results regardless of the frequency.

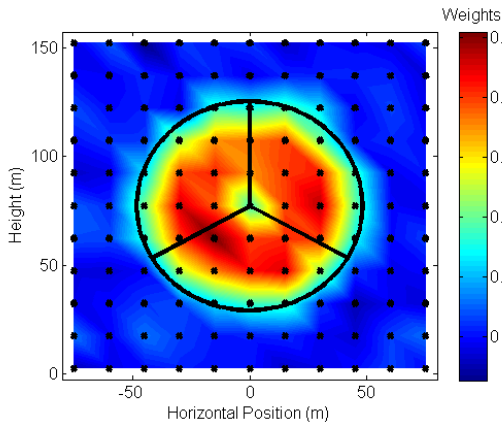
Figure 4.6 offers insight into what wind speeds affect the turbine dynamics. At low frequency, the grid points weighted heaviest are all of those inside the rotor disk. This makes sense because the definition of effective wind speed is the average wind speed across the rotor plane. The wind outside of the rotor disk does not interact with the blades and so cannot affect the turbine dynamics. Furthermore, the hub grid point and grid points near the blade tips are weighted less. The lower weight at the hub grid point makes sense because no lift is generated at the hub/blade roots. The blade tips may be weighted less due to tip losses. However, at higher frequencies, this organized weighting begins to break down. At about 5 rad/s (Figure 4.6 (e)), the weights start to take on more of a random pattern and by 60 rad/s, (Figure 4.6 (h)), the weighting is completely random. This may be because the higher frequency



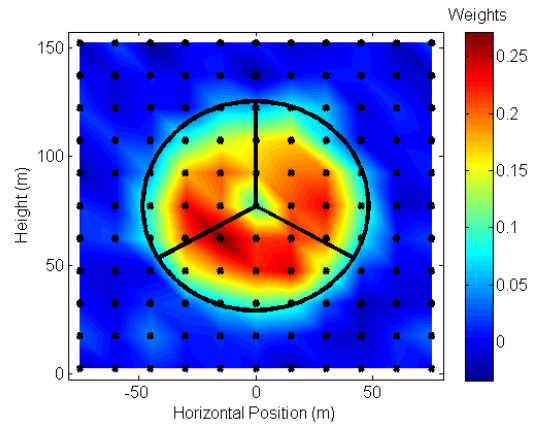
(a) Weights at 0.01 rad/s.



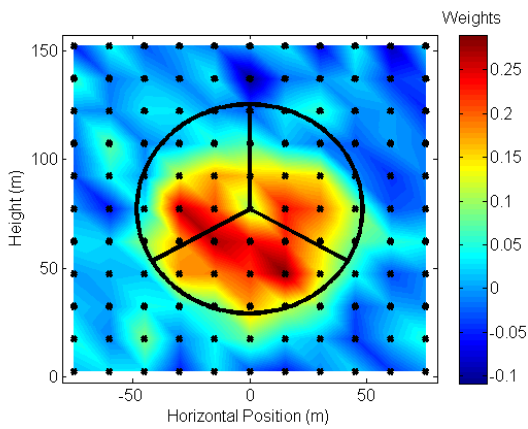
(b) Weights at 0.1 rad/s.



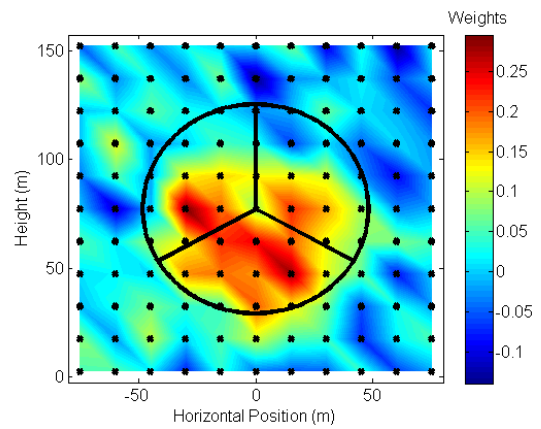
(c) Weights at 0.5 rad/s.



(d) Weights at 1 rad/s.



(e) Weights at 5 rad/s.



(f) Weights at 10 rad/s.

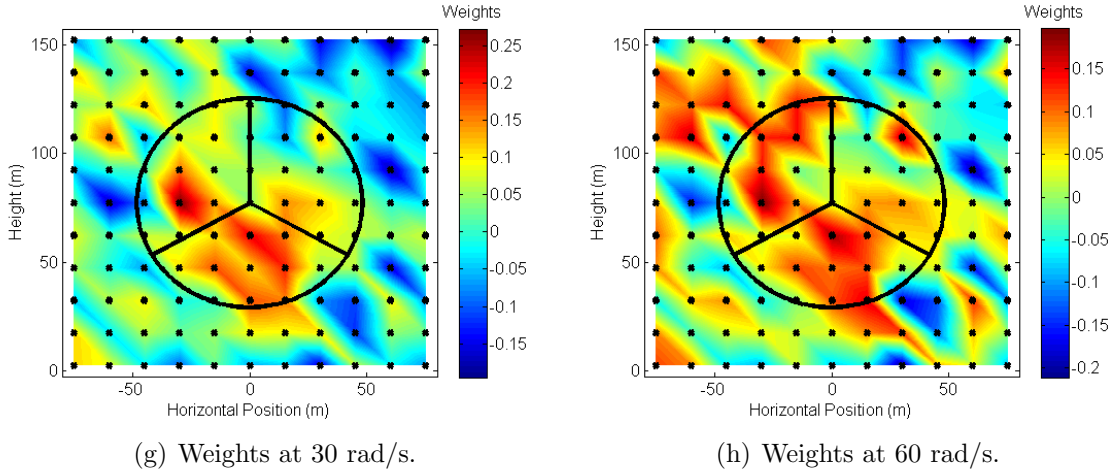


Figure 4.6: Weights, ν_1 , across the rotor plane at various frequencies for spatially varying wind input to FAST.

content of the wind varies rapidly and the large size of the turbine makes it slow to respond. Therefore, the high frequency content of the wind will have little to no effect on the turbine dynamics. The inability to identify a meaningful weight structure at higher frequencies may be what leads to inaccurate effective wind speed calculations seen in 4.5.

In order to obtain a more meaningful weight distribution across frequencies that could characterize the turbine’s behavior, the rotational nature of the wind turbine was considered. As the blades rotate about the hub, they are affected by the local wind characteristics only. In other words, at a given time step, the whole wind field is not acting on the turbine, only the grid points along the blade length. To take this fact into account, the wind field was rotated with the rotor as it rotated about the hub. However, this approach produced an identified model that was worse at matching the rotor speed and nacelle acceleration and did not produce a meaningful weight distribution.

By using the CLMOESP algorithm with a full wind field as the inputs, the algorithm was able to identify a turbine model capable of matching the measured results in the time domain. By performing a singular value decomposition on the $G(s)$ matrix, the notion of an effective wind speed was explored. This approach successfully identified the effective wind speed for a uniform flow field. Under spatially varying wind speed conditions, no meaningful way of calculating an effective wind speed could be identi-

fied, which makes sense because the blades are constantly rotating in space and being affected by different wind speeds. A direction of future work could include techniques for identifying a single effective wind speed and consistent weighting across frequencies. In addition, the weights indicated in 4.6 cannot realistically be measured so other future work could involve techniques for identifying smaller number of heavily weighted grid points. Alternatively, if a single effective wind speed cannot be found, a method for measuring multiple effective wind speeds should be investigated.

Chapter 5

Conclusion

System identification of wind turbines has the potential to open the doors for using more advanced control techniques to maximize power and minimize the loads on a wind turbine. This could lead to cutting turbine costs and helping maintain the rapid growth of wind energy worldwide.

There are many challenges associated with identification of wind turbines that were discussed in the previous sections. The primary source of these challenges are the spatial and temporal variation of the wind speed. The temporal variation causes the simple dynamic model to fail because the power coefficient is a steady-state notion that does not hold up in turbulent wind. Spatial wind variation complicates the identification process because there is not a single point at which the wind speed input can be measured to accurately identify a model.

The fact that the wind turbine must operate in closed-loop while collecting data for identification is an additional challenge. However, this and the temporal wind speed variation are accounted for by using more of a black box system identification algorithm called the CLMOESP. This algorithm allows the system to operate in closed-loop and makes no assumptions on the form of the system, doing away with the notion of a power coefficient.

Using the CLMOESP algorithm, a linear wind turbine model could be identified at various wind speeds as long as the wind speed was known (constant across the rotor plane). For more realistic operating conditions, the CLMOESP was used where the inputs were the wind speeds at many grid points across the rotor plane. Performing a

singular value decomposition of the identified $G(s)$ matrix showed which grid points were weighted the most to see where measurements should be taken for an effective wind speed. Although the algorithm was able to identify a model that matched the outputs in the time domain, a single effective wind speed did not materialize.

5.1 Future Work

There is large potential for future work using the results presented. First of which would be to investigate the notion of one effective wind speed. In practice, the wind speed across the rotor plane cannot be measured. Therefore, it would be useful to find a smaller number of effective wind speeds that might be able to be measured in practice.

Using the location of this effective wind speed or wind speeds, a LIDAR could be used with the Eolos Wind Energy Research Station to measure the wind speeds at the identified points in the rotor plane. The CLMOESP algorithm could then be used to perform system identification at a wide range of operating conditions to fully model the Clipper Liberty C96 research wind turbine.

Finally, the ultimate goal of this research is to use the identified system to perform advanced control design on the Clipper Liberty C96 wind turbine. Ideally, this advanced controller could be implemented on the C96 wind turbine. The identified model could then be verified by measuring expected versus actual performance.

The work presented here, combined with future work using data from a real wind turbine, can improve the capabilities of system identification of wind turbines and help continue the advancement of wind energy.

Bibliography

- [1] “Key Statistics of World Wind Energy Report 2013,” *13th World Wind Energy Conference*, 2014.
- [2] “EOLOS Wind Energy Research Consortium,” <http://www.eolos.umn.edu/>, May 2013.
- [3] “AWEA U.S. Wind Industry Annual Market Report Year Ending 2013,” January 2014.
- [4] Pao, L. Y. and Johnson, K. E., “Control of Wind Turbines,” *IEEE Control Systems*, Vol. 31, No. 2, March 2011, pp. 44–62.
- [5] Burton, T., Sharpe, D., Jenkins, N., and Bossanyi, E., *Wind Energy Handbook*, John Wiley & Sons, 1st ed., 2001.
- [6] Hassan, G., “Bladed Wind Turbine Design Software,” 2012.
- [7] “NWTC Computer-Aided Engineering Tools (FAST by Jason Jonkman, Ph.D.),” October 2013.
- [8] Ljung, L., *System Identification: Theory for the User*, Prentice-Hall, 2nd ed., 1999.
- [9] Iribas-Latour, M. and Landau, I.-D., “Identification in closed-loop operation of models for collective pitch robust controller design,” *Wind Energy*, Vol. 16, pp. 383–399.
- [10] van Baars, G. E. and Bongers, P. M. M., “Closed Loop System Identification of an Industrial Wind Turbine System: Experiment Design and First Validation Results,” *Proceedings of the 33rd Conference on Decision and Control*, 1994, pp. 625–630.

- [11] van der Veen, G., van Wingerden, J., Fleming, P., Scholbrock, A., and Verhaegen, M., “Global data-driven modeling of wind turbines in the presence of turbulence,” *Control Engineering Practice*, 2013.
- [12] van der Veen, G., van Wingerden, J.-W., and Verhaegen, M., “Data-Driven Modelling of Wind Turbines,” *Proceedings of the 2011 American Control Conference*, 2011, pp. 72–77.
- [13] Jelavic, M., Peric, N., and Petrovic, I., “Identification of Wind Turbine Model for Controller Design,” *Proceedings of the 12th International Power Electronics and Motion Control Conference*, 2006, pp. 1608–1613.
- [14] Verhaegen, M., Verdult, V., and Bergboer, N., “LTI System Identification Toolbox,” November 2012.
- [15] van der Veen, G., van Wingerden, J.-W., and Verhaegen, M., “Closed-loop MOESP subspace model identification with parametrisable disturbances,” *Proceedings of the 2010 49th IEEE Conference on Decision and Control*, 2010, pp. 2813–2818.
- [16] van der Veen, G., *Identification of wind energy systems*, Ph.D. thesis, Delft Center for Systems and Control, 2013.
- [17] van Overschee, P. and Moor, B. D., *Subspace Identification For Linear Systems: Theory, Implementation, Applications*, Kluwer Academic Publishers, 2nd ed., 1996.
- [18] Verhaegen, M., “Identification of the deterministic part of MIMO state space models given in innovations form from input-output data,” *Automatica*, Vol. 30, No. 1, 1994, pp. 61–74.
- [19] Jonkman, J. M. and Jr., M. L. B., “FAST User’s Guide,” Tech. Rep. NREL/EL-500-38230, National Renewable Energy Laboratory, August 2005.
- [20] Ostergaard, K. Z., Brath, P., and Stoustrup, J., “Estimation of effective wind speed,” *Journal of Physics: Conference Series*, Vol. 75, No. 1, 2007.
- [21] Knudsen, T., Bak, T., and Soltani, M., “Prediction models for wind speed at turbine locations in a wind farm,” *Wind Energy*, Vol. 14, No. 7, October 2011, pp. 877–894.

- [22] Odgaard, P. F., Damgaard, C., and Nielsen, R., “On-Line Estimation of Wind Turbine Power Coefficients Using Unknown Input Observers,” *Proceedings of the 17th IFAC World Congress*, 2008, pp. 10646–10651.
- [23] Monroy, A. and Alvarez-Icaza, L., “Real-time identification of wind turbine rotor power coefficient,” *Proceedings of the 45th IEEE Conference on Decision and Control*, 2006, pp. 3690–3695.
- [24] Salas-Cabrera, R., Mayo-Maldonado, J. C., Leon-Morales, J. D., Rosas-Caro, J. C., Garcia-Guendulain, C., Salas-Cabrera, N., Castillo-Ibarra, R., Gomez-Garcia, M., and Castillo-Gutierrez, R., “Real-time identification of wind turbine rotor power coefficient,” *Proceedings of the 20th IEEE International Conference on Electronics, Communications and Computer*, 2010, pp. 237–241.
- [25] Ma, X., Poulsen, N. K., and Bindner, H., “Estimation of wind speed in connection to a wind turbine,” Tech. Rep. IMM-Technical Report 1995-26, Technical University of Denmark, December 1995.
- [26] Leithead, W. E., “Effective wind speed models for simple wind turbine simulations,” *British Wind Energy Conference*, 1992, pp. 321–326.
- [27] Jonkman, B. J. and Kilcher, L., “TurbSim User’s Guide: Version 1.06.00,” Tech. Rep. NREL/TP-xxx-xxxx, National Renewable Energy Laboratory, September 2012.

Appendix A

Appendices

A.1 Eolos Database Search Algorithm

The algorithm below was used to discover extended time periods during which the Clipper Liberty C96 was in the desired operating conditions. In the code below, the algorithm is searching for any data set from 2013 where blade pitch is less than 1.05, wind direction is between 350 and 10 degrees (from the North), and the turbine state is equal to 8, meaning it is operating under normal conditions. This example will output any data series that meets these criteria and is longer than 1200 seconds (20 minutes).

```
SET TRANSACTION ISOLATION LEVEL READ UNCOMMITTED
; WITH BadRecords AS
(
SELECT
ROW_NUMBER() OVER(ORDER BY Record) AS RN,
HubSpd,
Timestamp
FROM
eolos.scada.Status
WHERE
Timestamp BETWEEN '2013-01-01 00:00:00.000' AND '2013-12-31 23:59:59.000'
AND (PitchPos1 > 1.05 OR WindDir > 10 OR WindDir < 350 OR TurbineState != 8)
),
```

```

Differences AS
(
SELECT
a.Timestamp,
ABS(DATEDIFF(second, a.Timestamp, b.Timestamp)) AS Diff
FROM
BadRecords a
INNER JOIN BadRecords b
ON a.RN = (b.RN+1)
)

SELECT
DATEADD(second, -Diff, Timestamp) AS StartTime,
Timestamp AS EndTime,
Diff
FROM
Differences
WHERE
Diff > 1200
ORDER BY
Diff

```